Asymmetric Optical Transitions Determine the Onset of Carrier Multiplication in Lead Chalcogenide Quantum Confined and Bulk Crystals

Spoor, Frank C.M.; Grimaldi, Gianluca; Delerue, Christophe; Evers, Wiel H.; Crisp, Ryan W.; Geiregat, Pieter; Hens, Zeger; Houtepen, Arjan J.; Siebbeles, Laurens D.A.

DOI
10.1021/acsnano.8b01530

Publication date
2018

Document Version
Final published version

Published in
ACS Nano

ACS NANO

Cite This: ACS Nano 2018, 12, 4796–4802

www.acsnano.org

ARTICLE

Asymmetric Optical Transitions Determine the Onset of Carrier Multiplication in Lead Chalcogenide Quantum Confined and Bulk Crystals

Frank C. M. Spoor,[†] Gianluca Grimaldi,[†] Christophe Delerue,[‡] Wiel H. Evers,[†] Ryan W. Crisp,[†] Pieter Geiregat,[§] Zeger Hens,[§] Arjan J. Houtepen,*[,†] and Laurens D. A. Siebbeles*[,†]

[†]Chemical Engineering Department, Delft University of Technology, Van der Maasweg 9, 2629 HZ Delft, The Netherlands

[‡]IEMN, Département ISEN, UMR CNRS, 59046 Lille Cedex, France

[§]Physics and Chemistry of Nanostructures, Ghent University, 9000 Ghent, Belgium

Supporting Information

ABSTRACT: **Carrier multiplication is a process in which one absorbed photon excites two or more electrons. This is of great promise to increase the efficiency of photovoltaic devices. Until now, the factors that determine the onset energy of carrier multiplication have not been convincingly explained. We show experimentally that the onset of carrier multiplication in lead chalcogenide quantum confined and bulk crystals is due to asymmetric optical transitions. In such transitions most of the photon energy in excess of the band gap is given to either the hole or the electron. The results are confirmed and explained by theoretical tight-binding calculations of the competition between impact ionization and carrier cooling. These results are a large step forward in understanding carrier multiplication and allow for a screening of materials with an onset of carrier multiplication close to twice the band gap energy. Such materials are of great interest for development of highly efficient photovoltaic devices.**

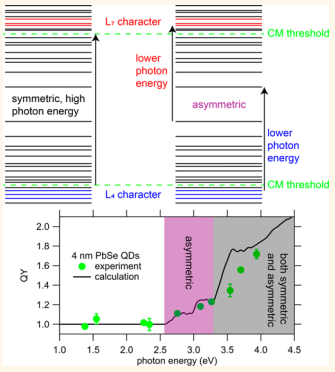

KEYWORDS: *quantum dot, carrier multiplication, carrier cooling, threshold energy, transient absorption spectroscopy, tight-binding calculations*

For solar cells, semiconductor quantum dots (QDs) are of interest due to inexpensive and facile synthesis and processing procedures using wet chemistry as well as desirable optical properties such as a size-tunable band gap, photostability, and the occurrence of efficient carrier multiplication (CM).[1−5] In the latter process, absorption of a single, high-energy photon leads to the creation of two or more electron−hole pairs. The onset of CM, which is the lowest photon energy for which CM occurs, is the most important aspect for enhancement of the photovoltaic efficiency in solar cells.[6] Ideally, this onset is at twice the band gap energy, limited only by energy conservation. In practice, the onset of CM is higher and depends on the size, shape, and composition of the material.[7] Significant research effort has been devoted to reducing the onset of CM by tuning these parameters.[8−12] The origin of the onset is however poorly understood, crippling the search for materials and structures with a lower onset of CM.

CM in lead chalcogenide (PbX, X = S, Se, Te) crystals is usually described in terms of a competition between impact ionization (II), the process in which a hot electron excites a second electron over the band gap, and other cooling channels.[13−17] These other cooling channels include emission of bulk-like PbX phonons, emission of surface related phonons, excitation of surface ligand vibrations, and trapping to surface states.[18−26] Typically only the highest valence and lowest conduction bands are considered. In our earlier work we have however shown that additional bands are important for absorption of high-energy photons and cooling of hot charge carriers in PbS and PbSe QDs.[27−29] At high photon energy where CM occurs, one should therefore take the entire band structure into account.

Here, we show that asymmetric optical transitions involving higher valence and conduction bands determine the onset of CM in PbX quantum confined and bulk crystals. Using tight-binding calculations we show that the asymmetric distribution of photon excess energy between the electron and hole explains the onset of CM. The asymmetric distribution is due to excitation of electronic states associated with the highest

Received: February 27, 2018
Accepted: April 17, 2018
Published: April 17, 2018

DOI: 10.1021/acsnano.8b01530
ACS Nano 2018, 12, 4796−4802

valence band to the second lowest conduction band or from the second highest valence band to the lowest conduction band. These processes are different from excitations in which the photon energy is distributed asymmetrically between charge carriers due to a large difference in effective masses (such as in InAs)[30] of the highest valence band and lowest conduction band, since higher bands are involved that can possibly lead to slower cooling or higher II rates. With this insight, the search for a material suitable to exploit CM can be directed at semiconductors with strong asymmetric optical transitions involving higher bands at two times the band gap energy.

RESULTS AND DISCUSSION

We have synthesized colloidal PbS and PbSe QDs of various sizes following the procedures of Cademartiri *et al.*[31] modified by Moreels *et al.*[32] and Steckel *et al.*[33] The size of the QDs was tuned by variation of the reaction time after injection of sulfur or selenium. The CM yield as a function of photon energy was measured using transient absorption (TA) spectroscopy with pump and probe laser pulses of 180 fs duration, as described previously.[27−29] The QD samples were stirred to prevent photocharging.[34] In Figure 1a we show a typical hyperspectral

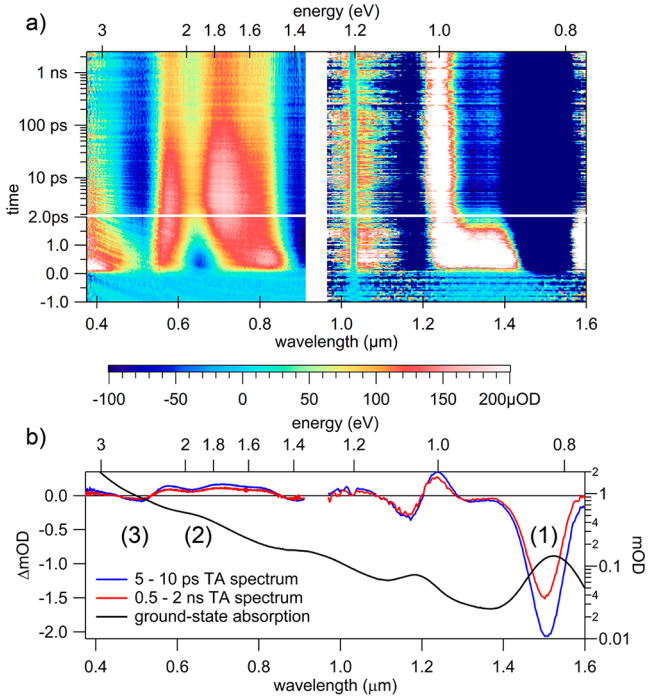

Figure 1. (a) Hyperspectral TA image for 4.8 nm PbSe QDs photoexcited at 3.5 eV (350 nm). (b) Time averaged spectra at 5−10 ps and 0.5−2 ns pump−probe delay, before and after Auger decay has taken place. The spectral features labeled 1−3 are discussed in the text.

TA image for 4.8 nm PbSe QDs with a band gap of 0.82 eV (1520 nm), photoexcited at 3.5 eV (350 nm). The image shows the change in absorption resulting from photoexcitation as a function of pump−probe delay time and probe wavelength. Initially hot charge carriers are created by absorption of photons with energy larger than the band gap. Subsequently they cool down through II or other cooling channels. Time averaged spectra at various delay times are shown in Figure 1b, where we highlight three spectral features paramount to this work.

At 5−10 ps pump−probe delay the hot charge carriers have cooled down to the band edge. Feature (1) in Figure 1b is the band edge bleach resulting from reduced ground-state absorption and stimulated emission due to the presence of band edge excitons. This bleach signal scales with the number of band edge excitons and is used to determine the CM yield.[35−37] The band edge bleach is reduced at 0.5−2 ns pump−probe delay, since Auger decay of multiple excitons has taken place, leaving at most a single cold exciton in each QD. Feature (2) in Figure 1b is a shift of the Σ_{5-6} transition,[27] while feature (3) in Figure 1b results from a bleach and shift of the high-energy L_{4-6} and L_{5-7} transitions.[28] These transitions are important when considering absorption of high-energy photons and cooling of hot charge carriers. They should therefore be included in a discussion of CM. The Σ_{5-6}, L_{4-6} and L_{5-7} transitions are indicated in the bulk band structure of PbSe and PbS in Figure 2a and 2b, with the bands involved numbered 4−7.

Determination of the CM characteristics in PbX QDs from transient absorption spectra is well-established and described in the Supporting Information (Figure S1).[35−37] The quantum yield (QY) is defined as the number of electron−hole pairs generated per absorbed photon. The QY data for PbSe and PbS QDs are shown in Figure 3a and 3b and in Figures S2 and S3 of the Supporting Information, as a function of photon energy normalized by the band gap. For high photon energies, the QY exceeds unity, due to the occurrence of CM. Within the error margin, the results agree well with the measurements of Ellingson *et al.*[36] and McGuire *et al.*[34] Following previous studies, we determine the CM threshold and CM efficiency from a linear fit to the QY data exceeding unity.[12,38,39] The energy at which this fit gives a QY equal to 1 is taken as the threshold of CM, while the slope of the line is the CM efficiency. Hence, the CM efficiency is the number of electron−hole pairs produced per unit normalized photon energy above the threshold. Note that the CM efficiency defined in this way is a simplification, since the QY does not necessarily increase linearly with photon energy, as we discuss below. We choose not to fit the model of Beard *et al.*[15] to our data, since it does not take into account any bands higher than those at the band edge, while we show here that higher bands determine the CM threshold. To study the relation between the Σ_{5-6}, L_{4-6}, and L_{5-7} transitions from Figure 2 and CM, their transition energies and the CM threshold are plotted *versus* the band gap energy, E_{bg}, in Figure 3 for PbSe (d) and PbS (d) quantum confined and bulk crystals.

From Figure 3a and 3b we observe that the dependence of the QY on normalized photon energy varies with the size of the QDs, showing an increase in CM threshold and efficiency with increasing QD size. The results are comparable for PbSe and PbS QDs. The latter is not surprising, since the bulk electronic band structures of PbSe and PbS are qualitatively similar, see Figure 2. From Figure 3c and 3d we observe that for all PbSe and PbS QDs, the CM threshold coincides with the L_{4-6} and L_{5-7} transition energies and lies well above the Σ_{5-6} transition energy. Moreover, the threshold in bulk PbSe and PbS crystals (taken from Pijpers *et al.*)[40] also coincides with the transitions. Interestingly, when we decrease the PbSe QD size to 1.3 nm such that the L_{4-6} and L_{5-7} transition energies are lower than twice the band gap energy, we measure no CM up to our highest photon energy of 4 eV, equal to 2.5 times the band gap energy for this PbSe QD size. Hence, these asymmetric optical transitions determine the CM threshold in both PbSe and PbS

DOI: 10.1021/acsnano.8b01530
ACS Nano 2018, 12, 4796−4802

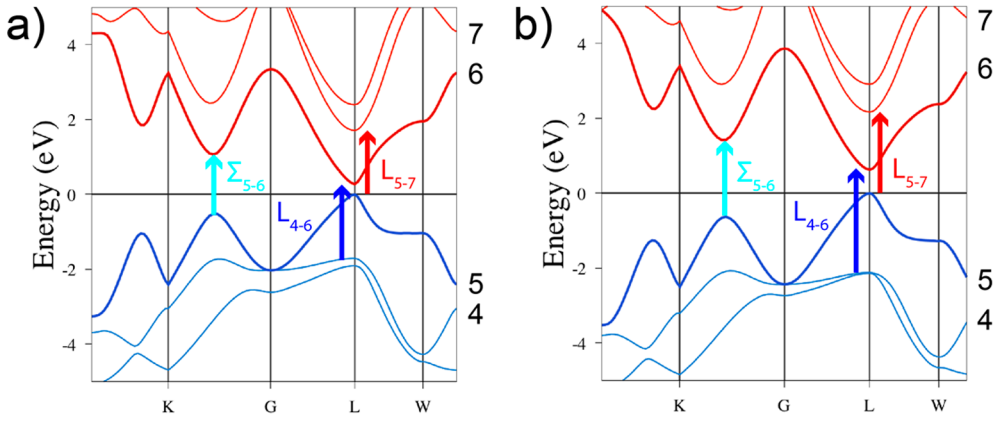

Figure 2. Bulk band structure of (a) PbSe and (b) PbS. The bands near the band gap are numbered 4−7 and the Σ_{5-6}, L_{4-6}, and L_{5-7} transitions are indicated.

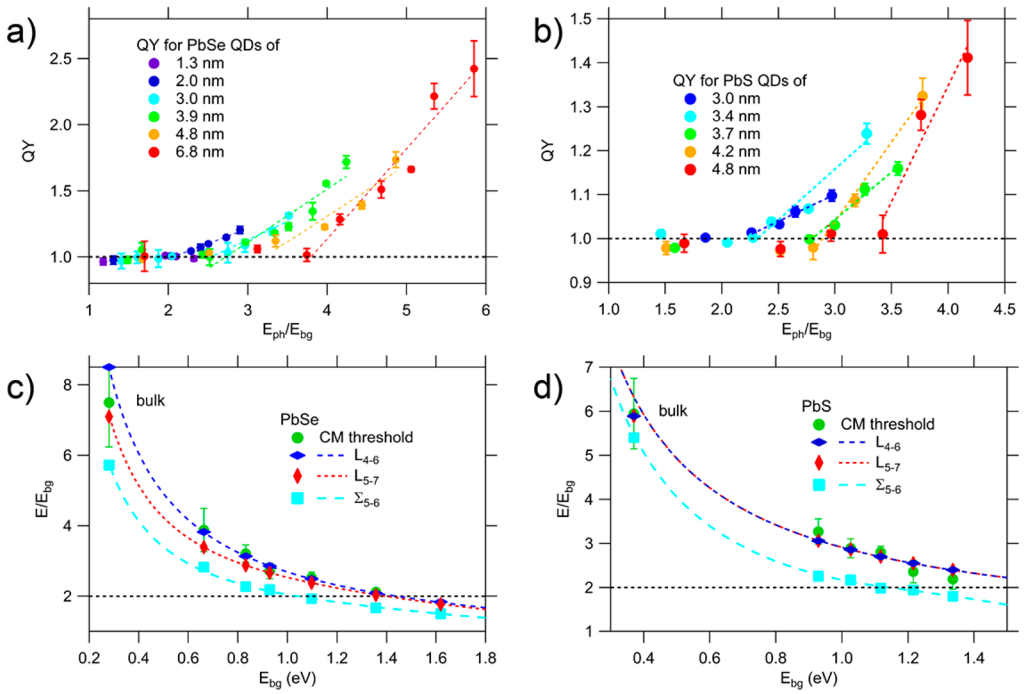

Figure 3. (a and b) QY as a function of photon energy normalized by the band gap energy for various sizes of PbSe and PbS QDs. (c and d) Normalized Σ_{5-6}, L_{4-6}, and L_{5-7} transition energies and the CM threshold as a function of band gap energy for PbSe and PbS quantum confined and bulk crystals. Bulk data were taken from the work of Pijpers *et al.*[40]

quantum confined and bulk crystals, while the energies of the band gap and of these asymmetric transitions depend on the size through quantum confinement.

We show the same data of Figure 3 as a function of absolute photon energy in the Supporting Information (Figure S4). We find that on an absolute photon energy scale, the CM threshold is highest for the smallest QDs and decreases with QD size. This is contrary to the increase of the CM threshold with QD size on a normalized photon energy scale. Interestingly, on both scales the CM threshold coincides with the occurrence of the asymmetric L_{4-6} and L_{5-7} transitions, highlighting again that it is not only the energy of the photon that matters but also the nature of the optical transition.

The question remains why the CM threshold in PbSe and PbS quantum confined and bulk crystals coincides with the L_{4-6} and L_{5-7} transitions. For photon energies lower than the L_{4-6}, L_{5-7} and Σ_{5-6} transition energies, electrons are photoexcited around the L-point from the highest valence band to the lowest conduction band (bands 5 and 6 in Figure 2). These transitions distribute the excess photon energy almost symmetrically between the electron and the hole, due to the similar effective masses of electrons and holes at the valence and conduction band edges.[41] In this case, a photon energy of at least three times the band gap energy would be required, so that the electron and the hole have sufficient excess energy to undergo CM.[42] As we have observed from Figure 3 however, the CM threshold can be at lower photon energy. For photon energies equal to or higher than the L_{4-6} and L_{5-7} transition energies, some electrons are photoexcited from the second highest valence band to the lowest conduction band (L_{4-6}) or from the highest valence band to the second lowest conduction band (L_{5-7}). In this case most of the excess photon energy can be transferred to either the hole (L_{4-6}) or the electron (L_{5-7}), allowing the CM threshold to be reduced toward two times the

DOI: 10.1021/acsnano.8b01530
ACS Nano 2018, 12, 4796−4802

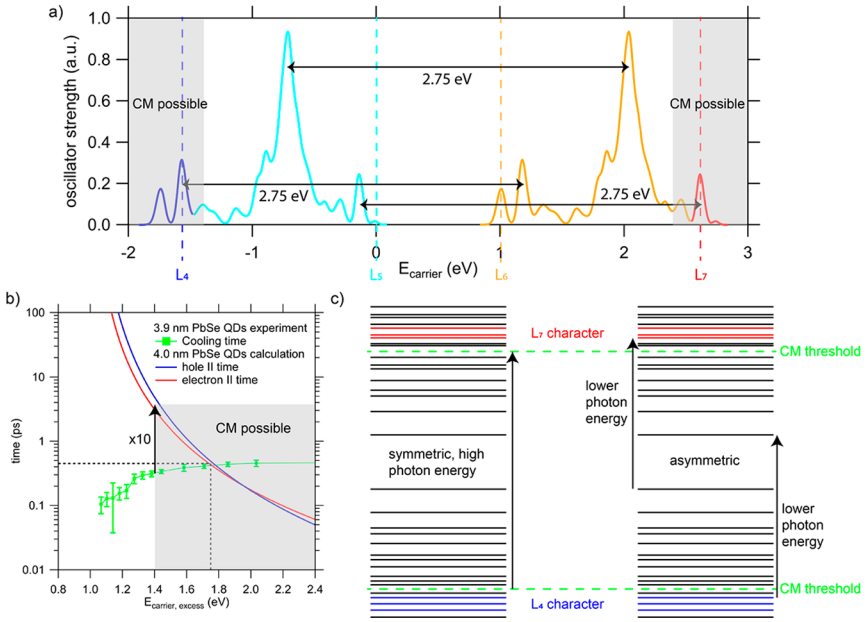

Figure 4. (a) Calculated optical oscillator strength as a function of carrier energy for absorption of a 2.75 eV photon for 4 nm PbSe QDs. The bands in which electrons and holes are created are indicated as well as the energy ranges (shaded areas) in which significant CM is possible considering the competition between II and cooling. (b) Calculated II time in 4 nm PbSe QDs and measured cooling time in 3.9 nm PbSe QDs, as a function of carrier excess energy. Below 1.4 eV carrier excess energy, the II time is more than 10 times higher than the cooling time and CM is negligible. Above 1.4 eV carrier excess energy, significant CM becomes possible. (c) Schematic PbSe QD electronic structure with CM thresholds indicated. The photon energy required to create electrons or holes above the CM threshold is much higher for symmetric transitions than for asymmetric transitions, as indicated by the arrows.

band gap energy. These considerations are discussed in terms of a bulk band structure. Care should be taken when QDs are studied, since the wave function of spatially confined electrons in QDs is a mixture of bulk electronic states.[43,44] Our previous work however showed that despite quantum confinement, there exist energy levels with large L_4 and L_7 character in PbSe QDs, allowing us to clearly identify L_{4-6} and L_{5-7} transitions in these systems.[28]

To get insight into the relation between the nature of optical transitions and the CM threshold in PbX quantum confined and bulk crystals, we performed tight-binding calculations on PbSe QDs with a diameter of 4 nm for which the calculated band gap is 1.0 eV (see Methods).[44−48] We first focus on the distribution of the excess photon energy between the electron and the hole at the lowest photon energy for which we measured a QY exceeding unity. This photon energy was 2.75 eV. Figure 4a shows the optical oscillator strength as a function of carrier energy for absorption of a 2.75 eV photon. The top of the valence band (L_5) is set to 0 eV and consequently the bottom of the conduction band (L_6) to 1 eV. We observe that most states are created with electron and hole energies distributed around 2.1 eV and −0.7 eV (1.1 and 0.7 eV excess energy), respectively, corresponding to almost symmetric transitions. Additionally, some electrons and holes are created with 2.6 eV and −1.6 eV of energy (1.6 eV excess energy in either case), respectively, due to the asymmetric L_{4-6} and L_{5-7} transitions. For significant CM to occur, a charge carrier not only requires sufficient excess energy but also its II rate must compete favorably with its cooling rate. We discuss below that although the electron has sufficient excess energy in the symmetric transitions, the asymmetric transitions are required to meet both conditions. The optical oscillator strength in Figure 4a agrees with the estimate in our previous work that the oscillator strength of the L_{4-6} and L_{5-7} transitions in PbSe QDs is approximately 1/8 of the oscillator strength at the band gap.[28]

To study the competition between II and cooling, we take the cooling time in 3.9 nm PbSe QDs from our previously published data on electron and hole cooling.[29] Figure 4b shows this cooling time together with the II time (1/rate) calculated for 4 nm PbSe QDs as a function of carrier excess energy.[14] The cooling time presented is essentially bulk-like, agreeing with literature on cooling of hot charge carriers.[29,49,50] The II time decreases much faster with carrier excess energy than the cooling time. This is caused by the strong increase in density of final states. We assume that for an II time more than 10 times larger than the cooling time, CM is negligible. From Figure 4b we observe that within this assumption, significant CM becomes possible for carrier excess energies above 1.4 eV, as indicated in the shaded areas of Figure 4a and 4b. At 1.4 eV carrier excess energy, we find an II time of 3.5 ps and corresponding II rate of 0.3 ps^{-1}. Despite the limits of correctly calculating energy differences with tight-binding theory, this approach allows us to identify the energetic onset of efficient CM.

Using Figure 4a and 4b we now find that at the experimentally determined CM threshold (at a photon energy of 2.75 eV), asymmetric L_{4-6} and L_{5-7} transitions occur, creating electrons and holes with sufficient excess energy to undergo CM and with an II rate that competes favorably with the cooling rate. Symmetric transitions will also contribute to II as soon as they create charge carriers with approximately 1.4 eV or more excess energy. This consideration is summarized in a schematic QD electronic structure in Figure 4c, where we show that the photon energy required to achieve sufficient carrier excess energy for CM is much higher for symmetric transitions than for asymmetric transitions.

DOI: 10.1021/acsnano.8b01530
ACS Nano 2018, 12, 4796−4802

Because of the steep decrease of the II time with carrier excess energy observed in Figure 4b, we can calculate an estimate of the QY by assuming that every charge carrier with sufficient excess energy (>1.0 eV) and an II rate that competes favorably with the cooling rate (>0.3 ps^{-1}, or an energy >1.4 eV) undergoes CM. For each photon energy, first the excess energy of electrons and holes for all possible optical transitions is calculated, together with the II rate as in Figure 4b. Next, if the II rate of both charge carriers is lower than 0.3 ps^{-1}, we set the QY to unity. If the II rate of either charge carrier for a specific transition is higher than 0.3 ps^{-1}, we assume that CM occurs and increases the QY by one. The total QY at a photon energy is then the average of the QYs for all possible optical transitions. In the Supporting Information (Figure S5) we show that experimentally we can estimate a lower limit to the II rate at the CM threshold of 0.3 ps^{-1}, equal to the II rate used here.

The calculated QY for 4 nm PbSe QDs is shown in Figure 5 as a function of photon energy for II by electrons, holes, and

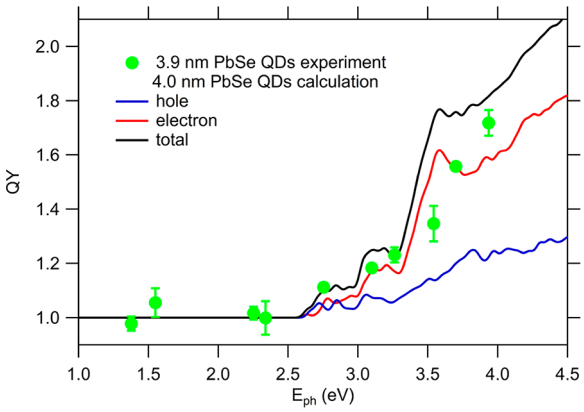

Figure 5. Calculated QY for 4 nm PbSe QDs when electrons and holes require an II rate of at least 0.3 ps^{-1}, compared to the experimental QY for 3.9 nm PbSe QDs, both as a function of photon energy.

both. The calculated total QY slightly overestimates the experimental results for 3.9 nm PbSe QDs, but has a similar shape. The larger theoretical result follows from our assumption that every charge carrier with an excess energy above 1.4 eV undergoes CM. In practice there is an energy range (~0.4 eV from Figure 4b) where significant competition between II and cooling occurs and not all charge carriers undergo CM. The QY starts rising at a photon energy of 2.6 eV, due to the occurrence of the L_{4-6} and L_{5-7} transitions. The calculated QY increases more rapidly with photon energy above approximately 3.5 eV, where symmetric transitions start contributing to II. Above the CM threshold, the calculated QY clearly does not increase linearly with photon energy. However, a linear fit is a reasonable approximation of the CM threshold and efficiency. The calculated QY in Figure 5 rises steeper with photon energy for electrons than for holes. Experimentally we are unable to make a distinction between the QY of electrons and holes, but we note that in our earlier work we experimentally determined that holes cool faster than electrons in PbSe QDs.[28,29] This effect would favor cooling in its competition with CM and therefore cause a more gentle increase of the QY with photon energy for holes.

We note that, besides the asymmetric division of photon energy, the nature of the states involved in the L_{4-6} and L_{5-7} transitions could play an important role in the CM process, due to the different character of the wave functions. Possibly hole cooling from the fourth to the fifth band or electron cooling from the seventh to the sixth band is slower than cooling within a band. It was recently shown that charge cooling between bands in silicon nanowires indeed is considerably slower than cooling within a single band.[51] Moreover, the matrix element for II could be larger for a transition between different bands, since this can occur by conservation of quasi-momentum (*i.e.*, vertical in *k*-space).[52] Both slower cooling and a larger matrix element for II would favor II in the competition with cooling. Further study of materials with small (*e.g.*, PbTe) or large differences in the electronic structure, especially of the higher bands, compared to PbSe and PbS could provide more insight in the involvement of these processes.

CONCLUSIONS AND OUTLOOK

We have shown experimentally that the CM threshold in PbX quantum confined and bulk crystals coincides with the L_{4-6} and L_{5-7} optical transitions. This can be understood in terms of an asymmetric distribution of photon energy between the electron and hole. The experimental findings of the QY of charge carriers produced by CM have been explained on the basis of theoretically calculated II rates and cooling times extracted from modeling experimental cooling data. A general understanding of CM based on considerations of the band structure of the material has been obtained, without the need to invoke special effects of quantum confinement. With these insights, we predict that a material will exhibit efficient CM when its band structure has the following properties. It requires a second conduction (valence) band at two times the band gap energy which can be populated due to a high oscillator strength and II should compete favorably with cooling. Quantum confinement is not necessary for these conditions, although it may be practical to achieve them. The discussed results allow for efficient screening of material candidates and rational engineering of CM efficient materials.

METHODS

Tight-Binding Calculations. The electronic structure of PbSe QDs was calculated in tight binding using, for each Pb or Se atom, a basis of $sp^3d^5s^*$ orbitals. The tight-binding parameters are taken from ref 48. They provide a band structure for bulk PbSe in excellent agreement with the GW calculations (many-body perturbation theory) of ref 47 taken as reference. Using these parameters, we predict band gaps of PbSe QDs *versus* size very close to those obtained using the tight-binding parameters of ref 44 that we employed in our previous studies (difference <0.1 eV). However, in the present work, we preferred to use the parameters of ref 48 because they put the minima of the second (L_7) and third (L_8) conduction bands in close agreement with the GW calculations, whereas the tight-binding model of ref 44 gives L_7 and L_8 conduction bands about 0.3 and 0.6 eV too low in energy, respectively.

The oscillator strengths for the optical transitions are calculated using the tight-binding electronic states following refs 45 and 46. In order to account for broadening effects in the optical spectra, each transition line is replaced by a Lorentzian (full width at half-maximum of 35 meV). The II rates and QY are calculated using the methodology described in ref 14.

ASSOCIATED CONTENT

Supporting Information

The Supporting Information is available free of charge on the ACS Publications website at DOI: 10.1021/acsnano.8b01530.

DOI: 10.1021/acsnano.8b01530
ACS Nano 2018, 12, 4796−4802

Method of determining CM from TA data (Figure S1). QY data for PbSe (Figure S2) and PbS (Figure S3) QDs. QY and CM threshold data of Figure 3 as a function of absolute photon energy (Figure S4). Experimental estimate of the II rate at the CM threshold (Figure S5) (PDF)

AUTHOR INFORMATION

Corresponding Authors

*E-mail: A.J.Houtepen@tudelft.nl.
*E-mail: L.D.A.Siebbeles@tudelft.nl.

ORCID

Christophe Delerue: 0000-0002-0427-3001
Zeger Hens: 0000-0002-7041-3375
Arjan J. Houtepen: 0000-0001-8328-443X
Laurens D. A. Siebbeles: 0000-0002-4812-7495

Author Contributions

F.C.M.S. and G.G. performed the measurements and analysis. W.H.E., R.W.C., and P.G. synthesized the quantum dots. C.D. performed the tight-binding calculations. Z.H., A.J.H., and L.D.A.S. managed the project.

Notes

The authors declare no competing financial interest.

ACKNOWLEDGMENTS

F.C.M.S. and L.D.A.S. were supported by the Dutch Foundation for Fundamental Research on Matter (FOM) with the project "Hot Electrons in Cool Nanocrystals". G.G., R.W.C., A.J.H., and L.D.A.S. were supported by STW (project no. 13903, Stable and Non-Toxic Nanocrystal Solar Cells).

REFERENCES

(1) Talapin, D. V.; Lee, J. S.; Kovalenko, M. V.; Shevchenko, E. V. Prospects of Colloidal Nanocrystals for Electronic and Optoelectronic Applications. *Chem. Rev.* **2010**, *110*, 389−458.

(2) Beard, M. C.; Luther, J. M.; Semonin, O. E.; Nozik, A. J. Third Generation Photovoltaics Based on Multiple Exciton Generation in Quantum Confined Semiconductors. *Acc. Chem. Res.* **2013**, *46*, 1252−1260.

(3) Smith, C.; Binks, D. Multiple Exciton Generation in Colloidal Nanocrystals. *Nanomaterials* **2014**, *4*, 19−45.

(4) Kershaw, S.; Rogach, A. Carrier Multiplication Mechanisms and Competing Processes in Colloidal Semiconductor Nanostructures. *Materials* **2017**, *10*, 1095.

(5) ten Cate, S.; Sandeep, C. S. S.; Liu, Y.; Law, M.; Kinge, S.; Houtepen, A. J.; Schins, J. M.; Siebbeles, L. D. A. Generating Free Charges by Carrier Multiplication in Quantum Dots for Highly Efficient Photovoltaics. *Acc. Chem. Res.* **2015**, *48*, 174−181.

(6) Hanna, M. C.; Nozik, A. J. Solar Conversion Efficiency of Photovoltaic and Photoelectrolysis Cells with Carrier Multiplication Absorbers. *J. Appl. Phys.* **2006**, *100*, 074510.

(7) Padilha, L. A.; Stewart, J. T.; Sandberg, R. L.; Bae, W. K.; Koh, W.-K.; Pietryga, J. M.; Klimov, V. I. Carrier Multiplication in Semiconductor Nanocrystals: Influence of Size, Shape, and Composition. *Acc. Chem. Res.* **2013**, *46*, 1261−1269.

(8) Luo, J.-W.; Franceschetti, A.; Zunger, A. Carrier Multiplication in Semiconductor Nanocrystals: Theoretical Screening of Candidate Materials Based on Band-Structure Effects. *Nano Lett.* **2008**, *8*, 3174−3181.

(9) Midgett, A. G.; Luther, J. M.; Stewart, J. T.; Smith, D. K.; Padilha, L. A.; Klimov, V. I.; Nozik, A. J.; Beard, M. C. Size and Composition Dependent Multiple Exciton Generation Efficiency in PbS, PbSe, and PbSxSe1−x Alloyed Quantum Dots. *Nano Lett.* **2013**, *13*, 3078−3085.

(10) Padilha, L. A.; Stewart, J. T.; Sandberg, R. L.; Bae, W. K.; Koh, W.-K.; Pietryga, J. M.; Klimov, V. I. Aspect Ratio Dependence of Auger Recombination and Carrier Multiplication in PbSe Nanorods. *Nano Lett.* **2013**, *13*, 1092−1099.

(11) Cirloganu, C. M.; Padilha, L. A.; Lin, Q.; Makarov, N. S.; Velizhanin, K. A.; Luo, H.; Robel, I.; Pietryga, J. M.; Klimov, V. I. Enhanced Carrier Multiplication in Engineerded Quasi-Type-II Quantum Dots. *Nat. Commun.* **2014**, *5*, 4148.

(12) Aerts, M.; Bielewicz, T.; Klinke, C.; Grozema, F. C.; Houtepen, A. J.; Schins, J. M.; Siebbeles, L. D. A. Highly Efficient Carrier Multiplication in PbS Nanosheets. *Nat. Commun.* **2014**, *5*, 3789.

(13) Franceschetti, A.; An, J. M.; Zunger, A. Impact Ionization Can Explain Carrier Multiplication in PbSe Quantum Dots. *Nano Lett.* **2006**, *6*, 2191−2195.

(14) Allan, G.; Delerue, C. Role of Impact Ionization in Multiple Exciton Generation in PbSe Nanocrystals. *Phys. Rev. B: Condens. Matter Mater. Phys.* **2006**, *73*, 205423.

(15) Beard, M. C.; Midgett, A. G.; Hanna, M. C.; Luther, J. M.; Hughes, B. K.; Nozik, A. J. Comparing Multiple Exciton Generation in Quantum Dots To Impact Ionization in Bulk Semiconductors: Implications for Enhancement of Solar Energy Conversion. *Nano Lett.* **2010**, *10*, 3019−3027.

(16) Stewart, J. T.; Padilha, L. A.; Qazilbash, M. M.; Pietryga, J. M.; Midgett, A. G.; Luther, J. M.; Beard, M. C.; Nozik, A. J.; Klimov, V. I. Comparison of Carrier Multiplication Yields in PbS and PbSe Nanocrystals: The Role of Competing Energy-Loss Processes. *Nano Lett.* **2012**, *12*, 622−628.

(17) Stewart, J. T.; Padilha, L. A.; Bae, W. K.; Koh, W.-K.; Pietryga, J. M.; Klimov, V. I. Carrier Multiplication in Quantum Dots within the Framework of Two Competing Energy Relaxation Mechanisms. *J. Phys. Chem. Lett.* **2013**, *4*, 2061−2068.

(18) Wehrenberg, B. L.; Wang, C.; Guyot-Sionnest, P. Interband and Intraband Optical Studies of PbSe Colloidal Quantum Dots. *J. Phys. Chem. B* **2002**, *106*, 10634−10640.

(19) Guyot-Sionnest, P.; Wehrenberg, B.; Yu, D. Intraband Relaxation in CdSe Nanocrystals and the Strong Influence of the Surface Ligands. *J. Chem. Phys.* **2005**, *123*, 074709.

(20) Cooney, R. R.; Sewall, S. L.; Anderson, K. E. H.; Dias, E. A.; Kambhampati, P. Breaking the Phonon Bottleneck for Holes in Semiconductor Quantum Dots. *Phys. Rev. Lett.* **2007**, *98*, 177403.

(21) Sagar, D. M.; Cooney, R. R.; Sewall, S. L.; Dias, E. A.; Barsan, M. M.; Butler, I. S.; Kambhampati, P. Size Dependent, State-Resolved Studies of Exciton-Phonon Couplings in Strongly Confined Semiconductor Quantum Dots. *Phys. Rev. B: Condens. Matter Mater. Phys.* **2008**, *77*, 235321.

(22) Kilina, S. V.; Kilin, D. S.; Prezhdo, O. V. Breaking the Phonon Bottleneck in PbSe and CdSe Quantum Dots: Time-Domain Density Functional Theory of Charge Carrier Relaxation. *ACS Nano* **2009**, *3*, 93−99.

(23) Peterson, M. D.; Cass, L. C.; Harris, R. D.; Edme, K.; Sung, K.; Weiss, E. A. The Role of Ligands in Determining the Exciton Relaxation Dynamics in Semiconductor Quantum Dots. *Annu. Rev. Phys. Chem.* **2014**, *65*, 317−339.

(24) Lifshitz, E. Evidence in Support of Exciton to Ligand Vibrational Coupling in Colloidal Quantum Dots. *J. Phys. Chem. Lett.* **2015**, *6*, 4336−4347.

(25) Smith, C. T.; Leontiadou, M. A.; Page, R.; O'Brien, P.; Binks, D. J. Ultrafast Charge Dynamics in Trap Free and Surface Trapping Colloidal Quantum Dots. *Adv. Sci.* **2015**, *2*, 1500088.

(26) Bozyigit, D.; Yazdani, N.; Yarema, M.; Yarema, O.; Lin, W. M. M.; Volk, S.; Vuttivorakulchai, K.; Luisier, M.; Juranyi, F.; Wood, V. Soft Surfaces of Nanomaterials Enable Strong Phonon Interactions. *Nature* **2016**, *531*, 618−622.

(27) Geiregat, P.; Delerue, C.; Justo, Y.; Aerts, M.; Spoor, F. C. M.; Van Thourhout, D.; Siebbeles, L. D. A.; Allan, G.; Houtepen, A. J.; Hens, Z. A Phonon Scattering Bottleneck for Carrier Cooling in Lead Chalcogenide Nanocrystals. *ACS Nano* **2015**, *9*, 778−788.

(28) Spoor, F. C. M.; Kunneman, L. T.; Evers, W. H.; Renaud, N.; Grozema, F. C.; Houtepen, A. J.; Siebbeles, L. D. A. Hole Cooling Is

DOI: 10.1021/acsnano.8b01530
ACS Nano 2018, 12, 4796−4802

Much Faster than Electron Cooling in PbSe Quantum Dots. *ACS Nano* **2016**, *10*, 695−703.
(29) Spoor, F. C. M.; Tomić, S.; Houtepen, A. J.; Siebbeles, L. D. A. Broadband Cooling Spectra of Hot Electrons and Holes in PbSe Quantum Dots. *ACS Nano* **2017**, *11*, 6286−6294.
(30) Schaller, R. D.; Pietryga, J. M.; Klimov, V. I. Carrier Multiplication in InAs Nanocrystal Quantum Dots with an Onset Defined by the Energy Conservation Limit. *Nano Lett.* **2007**, *7*, 3469−3476.
(31) Cademartiri, L.; Bertolotti, J.; Sapienza, R.; Wiersma, D. S.; von Freymann, G.; Ozin, G. A. Multigram Scale, Solventless, and Diffusion-Controlled Route to Highly Monodisperse PbS Nanocrystals. *J. Phys. Chem. B* **2006**, *110*, 671−673.
(32) Moreels, I.; Justo, Y.; De Geyter, B.; Haustraete, K.; Martins, J. C.; Hens, Z. Size-Tunable, Bright, and Stable PbS Quantum Dots: A Surface Chemistry Study. *ACS Nano* **2011**, *5*, 2004−2012.
(33) Steckel, J. S.; Yen, B. K.; Oertel, D. C.; Bawendi, M. G. On the Mechanism of Lead Chalcogenide Nanocrystal Formation. *J. Am. Chem. Soc.* **2006**, *128*, 13032−13033.
(34) McGuire, J. A.; Joo, J.; Pietryga, J. M.; Schaller, R. D.; Klimov, V. I. New Aspects of Carrier Multiplication in Semiconductor Nanocrystals. *Acc. Chem. Res.* **2008**, *41*, 1810−1819.
(35) Schaller, R. D.; Klimov, V. I. High Efficiency Carrier Multiplication in PbSe Nanocrystals: Implications for Solar Energy Conversion. *Phys. Rev. Lett.* **2004**, *92*, 186601.
(36) Ellingson, R. J.; Beard, M. C.; Johnson, J. C.; Yu, P.; Micic, O. I.; Nozik, A. J.; Shabaev, A.; Efros, A. L. Highly Efficient Multiple Exciton Generation in Colloidal PbSe and PbS Quantum Dots. *Nano Lett.* **2005**, *5*, 865−871.
(37) Trinh, M. T.; Houtepen, A. J.; Schins, J. M.; Hanrath, T.; Piris, J.; Knulst, W.; Goossens, A. P. L. M.; Siebbeles, L. D. A. In Spite of Recent Doubts Carrier Multiplication Does Occur in PbSe Nanocrystals. *Nano Lett.* **2008**, *8*, 1713−1718.
(38) Aerts, M.; Suchand Sandeep, C. S.; Gao, Y.; Savenije, T. J.; Schins, J. M.; Houtepen, A. J.; Kinge, S.; Siebbeles, L. D. A. Free Charges Produced by Carrier Multiplication in Strongly Coupled PbSe Quantum Dot Films. *Nano Lett.* **2011**, *11*, 4485−4489.
(39) Sandeep, C. S. S.; Cate, S. t.; Schins, J. M.; Savenije, T. J.; Liu, Y.; Law, M.; Kinge, S.; Houtepen, A. J.; Siebbeles, L. D. A. High Charge-Carrier Mobility Enables Exploration of Carrier Multiplication in Quantum-Dot Films. *Nat. Commun.* **2013**, *4*, 2360.
(40) Pijpers, J. J. H.; Ulbricht, R.; Tielrooij, K. J.; Osherov, A.; Golan, Y.; Delerue, C.; Allan, G.; Bonn, M. Assessment of Carrier-Multiplication Efficiency in Bulk PbSe and PbS. *Nat. Phys.* **2009**, *5*, 811−814.
(41) Landolt, H.; Börnstein, R.; *Landolt-Börnstein - Group III Condensed Matter*; Springer-Verlag: Berlin, 1998; Vol. *41*.
(42) Hanna, M. C.; Beard, M. C.; Nozik, A. J. Effect of Solar Concentration on the Thermodynamic Power Conversion Efficiency of Quantum-Dot Solar Cells Exhibiting Multiple Exciton Generation. *J. Phys. Chem. Lett.* **2012**, *3*, 2857−2862.
(43) An, J. M.; Franceschetti, A.; Dudiy, S. V.; Zunger, A. The Peculiar Electronic Structure of PbSe Quantum Dots. *Nano Lett.* **2006**, *6*, 2728−2735.
(44) Allan, G.; Delerue, C. Confinement Effects in PbSe Quantum Wells and Nanocrystals. *Phys. Rev. B: Condens. Matter Mater. Phys.* **2004**, *70*, 245321.
(45) Graf, M.; Vogl, P. Electromagnetic Fields and Dielectric Response in Empirical Tight-Binding Theory. *Phys. Rev. B: Condens. Matter Mater. Phys.* **1995**, *51*, 4940−4949.
(46) Delerue, C.; Lannoo, M. *Nanostructures: Theory and Modelling*; Springer-Verlag: Berlin, 2004.
(47) Svane, A.; Christensen, N. E.; Cardona, M.; Chantis, A. N.; van Schilfgaarde, M.; Kotani, T. Quasiparticle Self-Consistent GW Calculations for PbS, PbSe, and PbTe: Band Structure and Pressure Coefficients. *Phys. Rev. B: Condens. Matter Mater. Phys.* **2010**, *81*, 245120.
(48) Poddubny, A. N.; Nestoklon, M. O.; Goupalov, S. V. Anomalous Suppression of Valley Splittings in Lead Salt Nanocrystals Without Inversion Center. *Phys. Rev. B: Condens. Matter Mater. Phys.* **2012**, *86*, 035324.
(49) Cho, B.; Peters, W. K.; Hill, R. J.; Courtney, T. L.; Jonas, D. M. Bulklike Hot Carrier Dynamics in Lead Sulfide Quantum Dots. *Nano Lett.* **2010**, *10*, 2498−2505.
(50) Miaja-Avila, L.; Tritsch, J. R.; Wolcott, A.; Chan, W. L.; Nelson, C. A.; Zhu, X. Y. Direct Mapping of Hot-Electron Relaxation and Multiplication Dynamics in PbSe Quantum Dots. *Nano Lett.* **2012**, *12*, 1588−1591.
(51) Li, J.; Niquet, Y.-M.; Delerue, C. Complexity of the Hot Carrier Relaxation in Si Nanowires Compared to Bulk. *Phys. Rev. B: Condens. Matter Mater. Phys.* **2017**, *95*, 205401.
(52) Landsberg, P. T. *Recombination in Semiconductors*; Cambridge University Press: New York, 1991.

DOI: 10.1021/acsnano.8b01530
ACS Nano 2018, 12, 4796−4802